JOURNAL OF Applied Polymer SCIENCE

An ambipolar polymer additive for enhanced open circuit voltage in a bulk heterojunction solar cells

Mahmood Alam Khan, Yong Mook Kang
Department of Energy and Materials Engineering, Dongguk University-Seoul, Seoul, 100-715, Republic of Korea
Correspondence to: M. A. Khan (E-mail: alamkhan77@gmail.com) and Y. M. Kang (E-mail: dake1234@dongguk.edu)

ABSTRACT: Open circuit voltage (V_{OC}) of organic bulk heterojunction solar cell is extended by the addition of a 20 wt % of F8TBT, an ambipolar polymer in the active layer matrixes (P3HT:PCBM) and then spin casted (1000 rpm/30 s) in the optimized devices on the PEDOT:PSS layer of the ITO glass. A substantial increase in the open circuit voltage from approximately 0.61–0.88 V (44.26%) has been observed with slight increase in efficiency up to 1.91% in the fabricated devices. However, further increment of F8TBT content to 40 wt % reduces the photovoltaic efficiency and affects the J_{SC} values remarkably, possibly due the excess amount of resistance developed. The enhancement of V_{OC} is attributed to the ambipolar nature of F8TBT polymer which facilitates the generated electron and hole transfer at the respective electrodes, enhanced π–π^* conjugation in polymer matrix, a superior nanoscale separation, and better molecular conformation at the film interface, thus giving an ample opportunities to explore the impact of blending of materials rather than depositing a thin buffer layer by expensive vapor phase technologies. The details of electrical and microstructure characterization of the film were analyzed by AFM, SEM, UV–Vis, *J–V* characteristics, and EQE techniques. © 2015 Wiley Periodicals, Inc. J. Appl. Polym. Sci. **2016**, *133*, 43042.

KEYWORDS: applications; coatings; films; organic photovoltaic applications; surfaces and interfaces

Received 11 June 2015; accepted 4 October 2015
DOI: 10.1002/app.43042

INTRODUCTION

Organic photovoltaic (OPV) technology owing to their large absorption coefficients, ease of processing, light weight, solution processable techniques, and a very low cost compared with the inorganic counterparts make them a promising alternative candidate to the well-known conventional photovoltaics.[1–3] The key advancement in the OPVs have been made in the last decade were remarkable and a solar energy performances with notable efficiencies up to 9% were achieved,[4] resulting from the rigorous modifications in the solar cell structures such as choice of solvents,[5] thermal annealing,[6] using a low band gap polymers,[7] and entirely a new kind of acceptors.[8]

Fundamentally, the efficiencies in solar cells are calculated by using the obtained data values of J_{SC}, V_{OC}, and fill factors; and any enhancement in any one of the three value leads to a higher in efficiencies of the devices. Recently, several possible routes of efficiency improvement in OPVs have been devised and applied including the application of low band gap polymers[9] to harness maximum solar absorption to augment the J_{SC} values, using new electron acceptor whose absorption covers wide range of solar spectrum ($PC_{85}BM$),[10] application of optical spacers,[11] stacking of n-type and p-type buffer layers at various hierarchical position,[12] and forming a tandem type device structures.[13]

Till date, most of the research in OPV are focused on the enhancement in electrical conductivities (J_{SC}) such as doping PEDOT:PSS layer by mannitol,[14] LiF layers,[15] and stacking several kind of buffer layers before and after the active layer deposition which results in the excellent enhancement of J_{SC} values, and in literature an enhanced incident photon to electron conversion efficiencies covering up to 80% of visible spectrum have been documented.[16] Therefore it is less likely to harness furthermore the visible region spectrum and the efficiencies reported till date are far from commercialization. So the renewed strategies should be focused on the open circuit voltage enhancement in conjunction to the J_{SC} enhancement, however, increase in the V_{OC} was thought to be primarily limited for the organic solar cell which consist of P3HT:PCBM heterojunction, since the highest occupied molecular orbital (HOMO) and lowest unoccupied molecular orbital (LUMO) [$V_{OC} = \Delta E - 0.3$, where ΔE is difference between HOMO and LUMO] were thought to be responsible and control the open circuit voltage (V_{OC}).[17] However, it is reported that only HOMO–LUMO are not only the sole factor which can influence the V_{OC}, such as Kim *et al.* reported that inserting a 10 nm pentacene layer augmented V_{OC} up to 0.73 V.[18] Moreover, it shows that the increase in V_{OC} will not merely depends on the LUMO–HOMO of electron acceptor

and donor, simultaneously it also influenced by the superior electrode contacts, a thin buffer layer insertion and nanoscale morphologies of the active layers. In this regard we believe that the understanding and augmentation of V_{OC} will be an effective guideline for enhancing performances of organic solar cells which are less explored areas of organic solar cells.

F8TBT{poly[(9,9-dioctylfluorene)−2.7-diyl-alt-[4,7-bis(3-hexylthien-f-yl)−2,1,3-benzothiadiazole]-2′,2″-diyl]} possess an ambipolar characteristics and it has been demonstrated pioneering effects in the field-effect transistors[19] and have potential to transport both the electron and holes either by employing with the P3HT or CdSe materials.[20] Furthermore, this ambipolar compound is widely utilized in the light emitting diodes (LEDs) as a conventional (F8TBT-out/Ca/Al) and hybrid (ITO/ZnO/Cs_2CO_3/F8TBT-in) type structure for the LED characteristic improvement.[21] Despite of having such excellent optoelectronic properties in LEDs its application in the bulk heterojunction (BHJ) solar cells along with P3HT:PCBM active layer is hitherto not reported despite of its obvious advantage of ambipolar nature and the great possibility to transport excitons efficiently to the respective electrodes, besides its solubility in a myriad of organic solvents. Here in, we report a substantial enhancement of V_{OC} to a value of 0.88 V from normal BHJs of 0.61 V when applied in organic solar cell by blending a controlled amount 20 wt % (2 mg) of F8TBT in the active layer (P3HT:PCBM) matrixes in chloroform solvent and spin casting at 1000 rpm/30 s on the PEDOT:PSS layer.

EXPERIMENTAL

The [6,6]-Phenyl C_{61} butyric acid methyl ester (PCBM) and region-regular Poly(3-hexylthiophene-2,5-dilyl) (P3HT) with a reagent grade chemicals were purchased from the Aldrich company. Poly[(9,9-dioctylfluorene)−2,7-diyl-alt-[4,7-bis(3-hexylthien-5-yl)−2,1,3-benzothiadiazole]-2′,2″-diyl] (F8TBT) also purchased from Sigma-Aldrich. The chloroform solvent was obtained from the Junsei Chemicals. The BHJ polymer solar cell was prepared as follows. The ITO (resistivity 15 V/sq) glass was masked, etched, and cleaned with the detergent, ethanol, then ultrasonicated in acetone, and cleaned further with O_2 plasma (40 W, 7.5 × 10^{-5} Pa) for 10 min. The highly conducting poly(3,4-ethylenedioxylenethiophene):polystyrene sulphonic acid (PEDOT:PSS) purchased from Baytron (H. C. Stark), was then spin casted (3000 rpm for 50 s) over the ITO layer. After that the substrate was baked at 130°C for 20 min. Chloroform used as a solvent for the active layer in the BHJ. In the 1.0 mL of solvent the P3HT (10 mg) and PCBM (10 mg) were added in a 4 mL vial in the glove box then sonicated for 20 min to dissolve both homogeneously and then the solution was magnetically stirred for 48 h (aging). After that active layer was spin casted over the PEDOT:PSS layer (1000 rpm/30 s) then dried, however optimization of spin coating speed was also studied before the final device meant for additive applications. This is denoted as normal BHJ in the manuscript. For the ambipolar F8TBT blended BHJ, in the 1.0 mL of solvent P3HT (10 mg), PCBM (10 mg), and a 2 mg of F8TBT were added in a 4 mL vial simultaneously and rest the procedure was followed same as the normal BHJ. Then with the use of cotton bud we removed the P3HT:PCBM spill over at the PN electrodes. To make the cell more simple without utilization of the thin LiF layer, an Al (80 nm) electrode was deposited by thermal evaporation in vacuum at about 2 × 10^{-5} torr. Then post annealing were carried out in vacuum at 110°C for 15 min. The fabricated devices were characterized by the photocurrent–voltage (*J–V*) curves measurement (digital source meter; model 2400, Keithly) in conditions illumination (AM1.5G, 100 mW/cm^2; model ORIEL-Sol-3A, Newport) which was calibrated to 100 mM/cm^2 using a reference Si photodevice. Atomic force microscopy (AFM) in tapping mode in air by Nano Scope IIIa (Digital Instruments). The incident photon to current conversion efficiency (IPCE) by Inc. (model QEX7 series). Scanning electron microscope (SEM) images by (TESCAN MIRA LMH2). UV–Vis by Shimadzu UV-3600 spectrophotometer. Each devices having an active area of 0.02 cm^2.

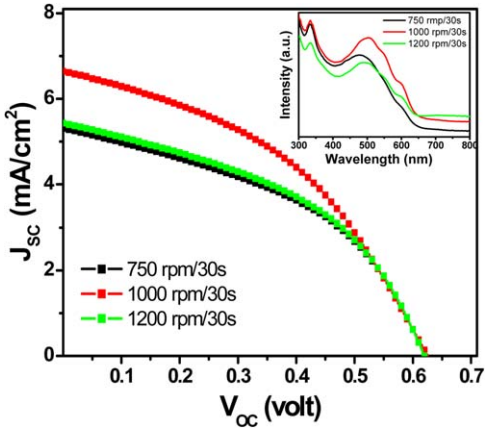

Figure 1. *J–V* characteristics measurement of fabricated devices with the optimization of spin coating speed in the BHJ solar cells. Inset shows the UV–Vis spectra of corresponding solar cells. [Color figure can be viewed in the online issue, which is available at wileyonlinelibrary.com.]

RESULTS AND DISCUSSION

Figure 1 shows the spin coating speed (rpm) optimization of the fabricated devices of BHJ solar cells with the *J–V* characteristics measured under the A.M.1.5G. It is clearly observed that the 1000 rpm/30 s shows the best efficiency of 1.7% (J_{SC} of 6.56 mA/cm^2 and V_{OC} of 0.62 V). Inset shows the UV–Vis spectra of the corresponding devices which also shows the consistency of the observed results. From the figure we can speculate that the spin coating speed of active layer are an important factor to achieve a good smoother film for the optimum efficiency in the BHJs. Since the J_{SC} of BHJ will rise with increase of film thickness ($I_d = \mu\tau E$, where μ is mobility, τ is life time, and *E* is electric field) due to more solar absorption on the other hand recombination increased with the film thickness resulting in electrical losses due to increased drift distances of the excitons, hence optimization of active film thickness by controlling the spinning speed and time are necessary for the better performance of the cell. Addition to film thickness, the phase separation is also optimized, since the BHJ solar cells are sensitive to small change in the parameters which affects the cell performance on small variations in the processing conditions. The post-annealing treatment applied in our solar cells which can augment the evaporation from the active layer by controlled demixing between the constituents resulting in the compact and

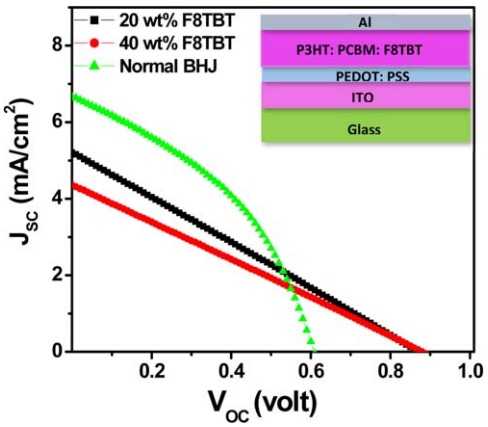

Figure 2. *J–V* characteristics measurement of fabricated devices with F8TBT blend and normal BHJ solar cells. Inset shows schematic diagram of the stacking layers. [Color figure can be viewed in the online issue, which is available at wileyonlinelibrary.com.]

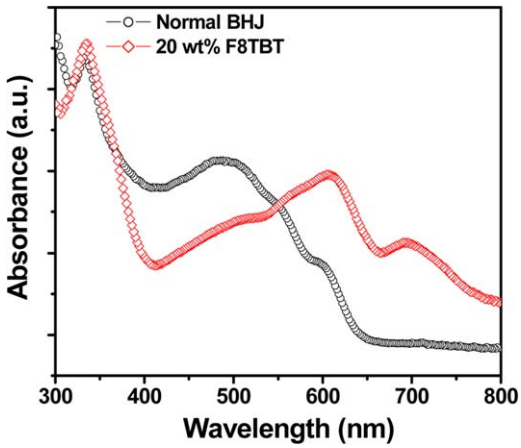

Figure 4. UV–Vis spectra measurement of fabricated devices with F8TBT blend and normal BHJ solar cells. [Color figure can be viewed in the online issue, which is available at wileyonlinelibrary.com.]

improved crystalline thin films hence the series resistance of this compact thin film may be decreased which contributed in the better performance of the fabricated devices.[22,23]

Figure 2 shows the *J–V* characteristics of the fabricated solar cell devices with controlled addition of F8TBT. It clearly indicates that the V_{OC} increases from 0.61 to 0.88 V from the normal BHJ solar cell structure, when the F8TBT was used a 20 wt % (of P3HT) blend as an additives and giving an efficiency of 1.91% from the 1.71% of normal BHJ solar cell structure. However, a slight decrease of J_{SC} value was observed from the normal BHJ (6.6 mA/cm^2) to blended BHJ (5.2 mA/cm^2). This could be attributed to the increase of the series resistance (R_S) in the blended solar cell device owing to the bulky polymeric {[4,7-bis(3-hexylthien-f-yl)−2,1,3-benzothiadiazole]-2′,2″-diyl, TBT} unit of F8TBT which affects the J_{SC} curve. It was further confirmed that the decreasing tendency of J_{SC} value were clearly observed in the devices when the blending amount of F8TBT additive were raised to a 40 wt % (F8TBT). The developed resistance by the addition of polymeric constituent may affects the mobility and carrier concentration which influences the J_{SC} value. It can be conjectured here that the nanoscale separation or aggregation of long chain polymers may also takes place where film is not completely spatially and equally distributed. Due to different in the densities of active layer and blended compounds the bulky group might settle down due to gravity effect at spin casting stage. The enhanced efficiency in 20 wt % additive may be ascribed to the intramolecular energy transfer of the excitons from the fluorine segment to the TBT unit (F8TBT) facilitating efficient transport. Inset in the figure shows the schematic diagram of the stacking layers in the solar cell device.

Figure 3 shows the analysis of external quantum efficiencies (EQE) of the normal BHJ and 20 wt % F8TBT blended organic solar cell devices. It can be clearly observed from the figure that the total quantum efficiency decrease of approximately 4% at the wavelength peaked at 502 nm have been observed in 20 wt % F8TBT blended (31%) from the normal fabricated BHJ (35%) structure. In our entire external quantum efficiency curve

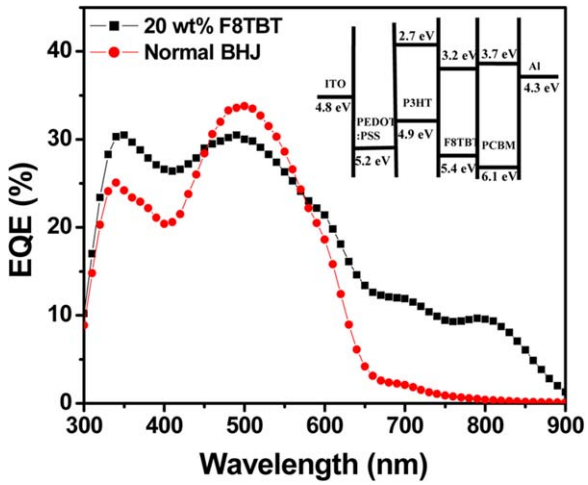

Figure 3. EQE characteristics measurement of fabricated devices with F8TBT blend and normal BHJ solar cells. Inset shows schematic band diagram of the HOMO and LUMO levels of components with F8TBT. [Color figure can be viewed in the online issue, which is available at wileyonlinelibrary.com.]

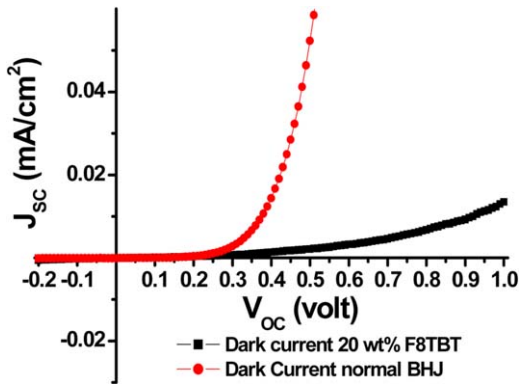

Figure 5. Shows the representative dark current diode characteristics for the fabricated 20 wt % F8TBT blended and normal BHJ devices. [Color figure can be viewed in the online issue, which is available at wileyonlinelibrary.com.]

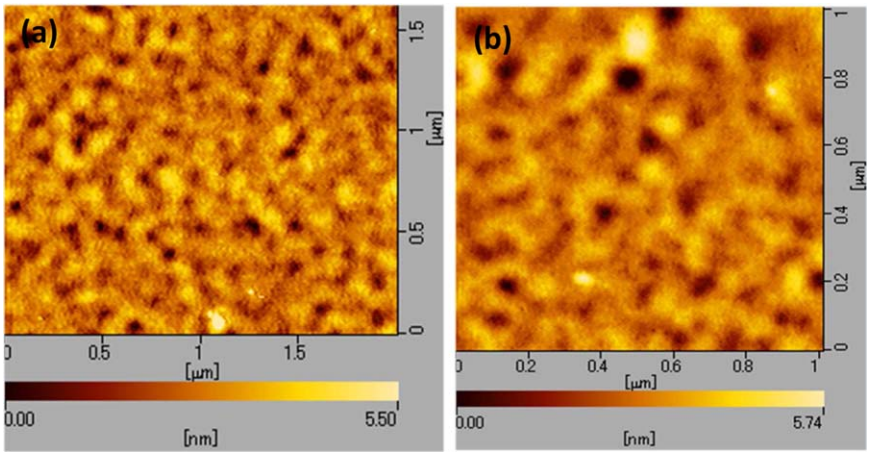

Figure 6. Surface topography measurement by atomic force microscopy (AFM) images the film (**a**) F8TBT blended BHJ and (**b**) normal P3HT:PCBM active layer BHJ. [Color figure can be viewed in the online issue, which is available at wileyonlinelibrary.com.]

mainly two kinds of peaks were observed, one narrow peaked at approximately 340 nm caused by PCBM layer and another broad hump peak centered at approximately 502 nm with a shoulder at approximately 700 nm, which is consistent with the main peak of the P3HT. However, it is interesting to note that an increase of quantum efficiencies at higher wavelength with hump peaked at 700–900 nm observed in only the F8TBT blended sample, such an extra absorbance hump was not observed in the normal BHJ. This additional wideness of the EQE could be the result of the better charge collection (exciton) efficiency due to ambipolar nature and an enhanced π–π^* conjugation in polymer matrix providing a sufficient percolation pathways toward the respective electrode due to the randomly distribution of F8TBT material in the bi-continuous active layer film in the range of exciton dissociation (10 nm). Inset of the figure shows a proposed interfaces energy band setup of HOMO–LUMO by using F8TBT in between active layer. The exciton are generated at the interface of P3HT:PCBM in the photoactive layer may provide better percolation pathway owing to its proximity and band matching with the active layers and also due to ambipolar nature. Figure 4 shows the UV–vis spectra of the normal and 20 wt % blended F8TBT BHJ solar cells. It shows that the intensity and shape of absorption features at approximately 330 nm peak position which arise due to HOMO–LUMO transitions of PCBM remains same and are undistinguishable in both the fabricated solar cell devices and at the longer wavelength feature from 460 to 620 nm are ascribed to be the P3HT polymer chains showing a better spectral vibrionic bands in the BHJ, however in the 20 wt % blended devices the P3HT peaks observed a bathochromic shift in the peak position at the wavelength of 603 nm (~104 nm) and light extends toward most of the visible spectrum up to the 670 nm, that shows a strong π–π^* absorption vibronic sidebands and the absorption peak hump at the 700–760 nm arises.

Figure 5 shows the representative dark current diode characteristics for the fabricated solar cell devices with the addition of 20 wt % F8TBT blend in active layer and a normal BHJ device prepared without the additives, it indicates clearly from the figure that the dark current response shows an expansion in V_{OC} (~0.35 V) where the modification of device with 20 wt % F8TBT has been carried out and normal BHJ depicting V_{OC} values (~0.20 V) on plotting the linear scale, nevertheless both the dark current analysis did not significantly short the electrical junction between anode and cathode and it shows that the diode characteristics with a clear expansion of open circuit voltage is consistent with the J–V measurement in the light.

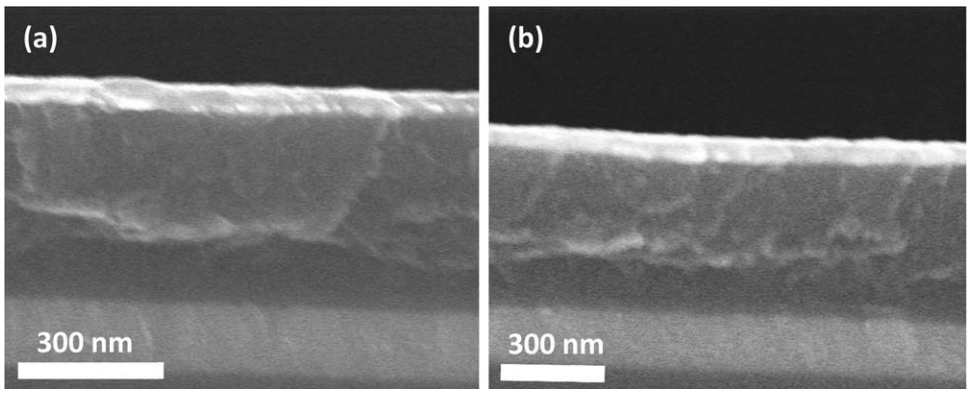

Figure 7. Cross sectional SEM measurement of fabricated devices with F8TBT blend (**a**) and normal (**b**) BHJ solar cells.

Figure 6 shows the representative topographic AFM of the sample blended with F8TBT (a) along with the active layer matrix and the normal BHJ (b) solar cell devices which were performed in this study. The images shows that the films were quite smooth in both the cases and not much different from each other in nano-scale length showing a good spatial arrangement of the films on spin casting and no phase segregation in domains were observed in the F8TBT blended sample which can be ascribed to the well miscibility in the chloroform solvent of ambipolar polymer. It can be also speculated that the roughness of the film do not have bumps, kinks rather a smoother films can be observed with the addition of 20 wt % F8TBT, where an enhanced miscibility with blending components and the proximity of active layer with ambipolymer polymer together results in better intermixing with the same solvent as of active layer shows a better results. It can also be seen from the figure that the nano domain up to approximately 6 nm roughness the dark and light spots were good enough to assess the good stacked film nature of our samples. Figure 7 shows the side-view cross sectional SEM images of the F8TBT blended (a) and normal (b) BHJ solar cells active layer films. It can be seen from the images that on the ITO substrate a clear demarcation of a thin layers of PEDOT:PSS observed and its thickness analyzed by the SEM at several position varies from approximately 50 nm to approximately 95 nm in the current study. The active layer is dense and also varied in thickness as average approximately 300 nm in our samples. It can be conjectured that there were no PCBM:P3HT or F8TBT particle segregation in the film interface and generally the films are homogenous and smooth, also there is not much microcrystal difference in the films between both the samples in normal as well as blended BHJ, respectively.

The charge generation in donor polymer-acceptor fullerene (P3HT:PCBM) interface strongly involves and influenced by the energetic landscape[24] and how well the coupling of electronic states interacts with *p–n* junctions that strongly affects the cell microstructure and obviously the efficiency, the factors such as donor–acceptor interactions, molecular orientation, and their packing along with the molecular conformation at the interface of the active layer films may causes interfacial charge deviation from the probable approximations. Since F8TBT consist of the F8, fluorine chain, and 4,7-bis(3-hexylthien-f-yl)−2,1,3-benzothiadiazole units which have low band gap characteristics and when these F8TBT blended with P3HT:PCBM active layer in a control dosages (20 wt %), an enhanced π–π^* conjugation in polymer matrix may lead to a red shift (as shown in EQE) which increased the exciton trap and facilitates the intermolecular energy transfer from fluorine segment to the TBT unit and successively to the electrodes leading to reduced decay constant and lowering the effective recombination, thus enhancing the efficiency. Furthermore, the energy level of F8TBT (HOMO- = 5.37 eV and LUMO = 3.15 eV) is a midway between the donor P3HT (HOMO = 4.9 eV and LUMO = 2.7eV) and acceptor PCBM (HOMO = 6.0 eV and LUMO = 4.2 eV) which favors energetically well distribution of generated charge transfer and percolation toward the respective electrodes. The inherent ambipolar nature of F8TBT which can acts as electron donor and hole transporter[25] can be exploited well in the BHJ solar cells since the dissociated excitons are well separated and owing to their nature of hole and electron transport and the proximity of F8TBT with P3HT:PCBM a better percolation pathway is developed and efficiency enhancement is observed. Moreover, a well nanoscale spatial distribution of F8TBT in whole the active layer may hop the excitons toward the respective electrodes.

CONCLUSION

Open circuit voltage of organic BHJ solar cell is enhanced by blending a 20 wt % of F8TBT additive in the active layer matrix (P3HT:PCBM) by spin casting on PEDOT:PSS layer at the optimized coating (1000 rpm/30 s). A substantial increase in the open circuit voltage 0.61–0.88 V has been observed with the increase in efficiency to 1.91% from 1.71%. However, increase of ambipolar F8TBT amount to 40 wt % affects the J_{SC} value but does not affect the V_{OC} of the cell. From the EQE observation it was found that wide range up to 700–900 nm absorption observed which was not observed in normal BHJ solar cells, thus this study shows a simple, inexpensive method of blending polymers with active layers to enhance parameters (V_{OC}) to augment the efficiency. It can be also speculated that the deposition of thin buffer layers by expensive vapor phase technologies can be also replaced by the wide intermixing soluble polymers in the active layers in the range of excitons (~10 nm) in organic solar cells.

ACKNOWLEDGMENTS

We greatly acknowledge to Dongguk University, Seoul for selecting Dr. Khan as a faculty position

REFERENCES

1. Heegar, A. J. *Adv. Mater.* **2014**, *26*, 10.
2. Vandewal, K.; Himmelberger, H.; Salleo, A. *Macromolecules* **2013**, *46*, 6379.
3. Park, S. H.; Roy, A.; Beaupre, S.; Cho, S.; Coates, N.; Moon, J. S.; Moses, D.; Lee, M. K.; Heeger, A. J. *Nat. Photon.* **2009**, *3*, 297.
4. Service, R. F. *Science* **2011**, *332*, 293.
5. Shaheen, S. E.; Brabec, C. J.; Sariciftci, N. S.; Padinger, F.; Fromherz, T.; Hummelen, J. C. *Appl. Phys. Lett.* **2001**, *78*, 841.
6. Li, G.; Shrotriya, V.; Huang, J.; Yao, Y.; Moriarty, T.; Emery, K.; Yang, Y. *Nat. Mater.* **2005**, *4*, 864.
7. Blouin, N.; Michaud, A.; Gendron, D.; Wakim, S.; Blair, E.; Neagu-Plesu, R.; Belletete, M.; Durocher, G.; Tao, Y.; Leclerc, M. *J. Am. Chem. Soc.* **2008**, *130*, 732.
8. Lenes, M.; Wetzelaer, G. A. H.; Kooistra, F. B.; Veenstra, S. C.; Hummelen, J. C.; Blom, P. W. M. *Adv. Mater.* **2008**, *20*, 2116.
9. Moon, J. S.; Jo, J.; Heeger, A. J. *Adv. Energy Mater.* **2012**, *2*, 304.
10. Kooistra, F. B.; Mihailetchi, V. D.; Popescu, L. M.; Kronholm, D.; Blom, P. M.; Hummelen, J. C. *Chem. Mater.* **2006**, *18*, 3068.

11. Kim, J. Y.; Kim, S. H.; Lee, H.; Lee, K.; Ma, W.; Gong, X.; Heeger, A. J. *Adv. Mater.* **2006**, *18*, 572.
12. Wei, Q. S.; Nishizawa, T.; Tajima, K.; Hashimoto, K. *Adv. Mater.* **2008**, *20*, 2211.
13. You, J.; Dou, L.; Hong, Z.; Li, G.; Yang, Y. *Prog. Polym. Sci.* **2013**, *38*, 1909.
14. Ko, C. J.; Lin, Y. K.; Chen, F. C.; Chu, C. W. *Appl. Phys. Lett.* **2007**, *90*, 063509.
15. Hung, L. S.; Tang, C. W.; Mason, M. G. *Appl. Phys. Lett.* **1997**, *70*, 152.
16. Kim, Y.; Cook, S.; Tuladhar, S. M.; Choulis, S. A.; Nelson, J.; Durrant, J. R.; Bradley, D. D. C.; Giles, M.; McCulloch, I.; Ha, C. H.; Ree, M. *Nat. Mater.* **2006**, *5*, 197.
17. Denhler, G.; Scharber, M. C.; Brabec, C. J. *Adv. Mater.* **2009**, *21*, 1323.
18. Kim, J. H.; Huh, S. Y.; Kim, T.; Lee, H. *Appl. Phys. Lett.* **2008**, *93*, 143305.
19. Hou, Q.; Xu, Y.; Yang, W.; Yuan, M.; Peng, J.; Cao, Y. *J. Mater. Chem.* **2002**, *12*, 2887.
20. Wang, P.; Abrusci, A.; Wong, H. M. P.; Svensson, M.; Andersson, M.; Greenham, N. C. *Nano Lett.* **2006**, *6*, 1789.
21. Lu, L. P.; Kabra, D.; Johnson, K.; Friend, R. H. *Adv. Funct. Mater.* **2012**, *11*, 144.
22. Reyes-Reyes, M.; Kim, K.; Carroll, D. L. *Appl. Phys. Lett.* **2005**, *87*, 083506.
23. Chu, C. W.; Yang, H. C.; Hou, W. J.; Huang, Li, G.; Yang, Y. *Appl. Phys. Lett.* **2008**, *92*, 103306.
24. Mc Neill, C. R. *Energy Environ. Sci.* **2012**, *5*, 5653.
25. Shi, C.; Yao, Y.; Yang, Y.; Pei, Q. *J. Am. Chem. Soc.* **2006**, *128*, 8980.